

Three-dimensional Intralunate Arteries Visualization with Red Lead (Pb_3O_4) Angiography

Zi-Run Xiao¹, Wei-Guang Zhang², Ge Xiong¹, You-Le Zhang¹

¹Department of Hand Surgery, Beijing Jishuitan Hospital, Beijing 100035, China

²Department of Anatomy and Histology, Peking University Health Science Center, Beijing 100191, China

Zi-Run Xiao and Wei-Guang Zhang contributed equally to this work.

Zi-Run Xiao now works at Department of Orthopaedic Surgery, PLA 91st Central Hospital.

Abstract

Background: The etiology of Kienböck's disease is controversial, and the blood supply is a possible pathogenic factor. The red lead (Pb_3O_4) angiography with micro-computed tomography (micro-CT) of lunate to investigate intralunate arteries has rarely been reported. This study aimed to investigate a new, reasonable, and simplified technique to study the intraosseous arterial pattern of normal lunates.

Methods: This study investigated the intraosseous arterial pattern of six normal cadaveric lunates through Pb_3O_4 injection and three-dimensional reconstruction with micro-CT. The intraosseous arteries of all specimens were clearly enhanced. The data of enhanced arteries and nutrient foramina were shown as median (Q_1 , Q_3) and analyzed with Wilcoxon signed-rank test.

Results: The mean number of total nutrient foramina was 2.00 (1.75, 2.00) on the palmar side and 3.50 (2.50, 4.25) on the dorsal side. The number with enhanced arteries on the palmar side was 1.00 (0.75, 2.00) and on the dorsal side was 3.50 (1.75, 4.00). There were no significant differences between the number of nutrient foramina on the palmar and dorsal sides of the lunates, no matter the total number or enhanced arteries. The intraosseous arterial pattern in normal lunates can be classified into three types: the dominate stems from the palmar side, from the dorsal side, and from both sides with anastomosis.

Conclusions: The Pb_3O_4 angiography with micro-CT is a simplified, quicker, and reliable method to study intraosseous arteries.

Key words: Intralunate Arteries; Micro-computed Tomography; Normal Lunates; Red Lead Angiography

INTRODUCTION

The etiology of Kienböck's disease (KD) is still controversial, and it is believed that blood supply of lunate is a core pathogeny of KD. The study of intraosseous arteries of the lunate will help to reveal the arterial anatomic factor of KD. Previous researchers studied the intraosseous vessel pattern by the way of arterial injection and the Spalteholz method, making the lunate transparent.^[1,2] However, the Spalteholz method is difficult to perform because of its numerous steps and long experimental time, which is sometimes up to 6 weeks. The first detailed study about circulation was performed by Manchot and reappraised by Salmon.^[3,4] Red lead (Pb_3O_4) injection described as the "gold standard" for anatomic study of microcirculation is the most popular method for visualization of the finest microvascular networks.^[4,5] In the recent decades, micro-computed tomography (micro-CT)

is used to study the microstructure of samples, and several researchers have used it to study the microstructure of the trabecular bone of the lunate.^[6-10] However, few studies on the intraosseous arterial pattern in lunates with micro-CT have been reported. We are trying to develop a new method to study the intraosseous arterial pattern of the lunate. The objective of this study was to introduce a new, reasonable, and more simplified technique to study the intraosseous arterial pattern of normal lunates with Pb_3O_4 arterial injection and micro-CT.

Address for correspondence: Dr. Ge Xiong,
Department of Hand Surgery, Beijing Jishuitan Hospital,
Beijing 100035, China
E-Mail: dr_xiongge@hotmail.com

This is an open access article distributed under the terms of the Creative Commons Attribution-NonCommercial-ShareAlike 3.0 License, which allows others to remix, tweak, and build upon the work non-commercially, as long as the author is credited and the new creations are licensed under the identical terms.

For reprints contact: reprints@medknow.com

© 2017 Chinese Medical Journal | Produced by Wolters Kluwer - Medknow

Received: 17-03-2017 **Edited by:** Yuan-Yuan Ji
How to cite this article: Xiao ZR, Zhang WG, Xiong G, Zhang YL. Three-dimensional Intralunate Arteries Visualization with Red Lead (Pb_3O_4) Angiography. Chin Med J 2017;130:2575-8.

Access this article online

Quick Response Code:



Website:
www.cmj.org

DOI:
10.4103/0366-6999.213909

METHODS

Ethical approval

The study was conducted in accordance with the *Declaration of Helsinki* and was approved by the Local Ethics Committee of Beijing Jishuitan Hospital (No. 201707-17).

Specimen handling

Sixty grams of Pb_3O_4 powder (Zhengzhou Chunming Trading Co., Ltd., China) was ground, filtered with a 300 mesh screen (diameter of about 48 μm), and divided into three equal parts. Each part was mixed with 10, 20, or 30 ml of turpentine, to produce three suspensions.

Six fresh cadaver upper limbs from three donors (a 55-year-old female, a 60-year-old male, and a 65-year-old male), assessed by X-ray to exclude diseased lunates, were studied. The limbs were thawed completely at room temperature if they had been frozen. The limbs were amputated at the level of proximal humeri. The brachial artery of each limb was dissected and then cut in the intermuscular groove of the biceps brachii at the level of the middle upper arm. A glass tube was inserted into the distal end of the brachial artery (the other end of the glass tube was connected with a rubber tube) and fixed with thread. To avoid air embolisms, a syringe was inserted into the rubber tube and slowly withdrawn, forming a negative pressure in the artery. Then, the rubber tube was clamped with forceps.

The Pb_3O_4 suspensions were injected into the brachial artery from a low concentration to a high concentration until the tips of fingers turned red. Then, the rubber tube was clamped with forceps and the artery was ligatured. All limbs were fixed in 10% formalin for 48 h.

Micro-computed tomography image processing

After fixation, the whole lunate was removed, and the soft tissue around the lunate was stripped as much as possible. All specimens were scanned with micro-CT (SkyScan 1172, Belgium; Scanning conditions: 100 kV, 90 μA , and resolution 12 μm) and three-dimensional (3D) images were reconstructed.

The reconstructed images were converted into the DICOM format and loaded with Mimics Research software (Materialise NV, Belgium, Platform: 17.0.0.435). By observing the nutrient foramina (a kind of tubular passage on cortex) on palmar and dorsal sides of the lunate images layer by layer, the number of nutrient foramina with/without enhanced arteries was recorded [Figure 1]. 3D models of enhanced arteries and the whole lunate were reconstructed. The enhancement of the arteries and the continuity of injected arteries was evaluated. Furthermore, the intraosseous arterial pattern could be observed from different directions and could be recorded.

Statistical analysis

The number of palmar/dorsal nutrient foramina was shown as median (Q_1 , Q_3) and analyzed with the Wilcoxon signed-rank test using SPSS Statistics software (IBM Corp. Version 19.0.

Armonk, NY, USA). A value of $P < 0.05$ was considered statistically significant.

RESULTS

Results of nutrient foramina

There were a total of 11 nutrient foramina on the palmar side of the specimens and four of them had no enhanced arteries. There were a total of 20 nutrient foramina on the dorsal side of the specimens and two of them had no enhanced arteries. The mean number of total nutrient foramina was 2.00 (1.75, 2.00) on the palmar side and 3.50 (2.50, 4.25) on the dorsal side. For the nutrient foramina with enhanced arteries, the number on the palmar side was 1.00 (0.75, 2.00) and on dorsal side was 3.50 (1.75, 4.00). However, no matter the total number of nutrient foramina ($Z = -1.807$, $P = 0.071$) or number of nutrient foramina with enhanced arteries ($Z = -1.913$, $P = 0.056$) between palmar and dorsal sides, there were no significant differences [Table 1].

Intraosseous vascular morphology

The intraosseous arteries in all lunates were enhanced with a clear configuration. Although there were some interrupted sites, the interrupted arteries could be regarded as the same artery depending on the direction of the arteries in the 3D or 2D images. We verified three types of Lee's classification^[1] for the intraosseous arteries of lunates. Type A (2/6 specimens) was the pattern with the arterial stems from the palmar side [Figure 2]. Type B (1/6 specimens) was the pattern with the stems from the dorsal side [Figure 3]. The arterial stems in Type C (3/6 specimens) were from both sides

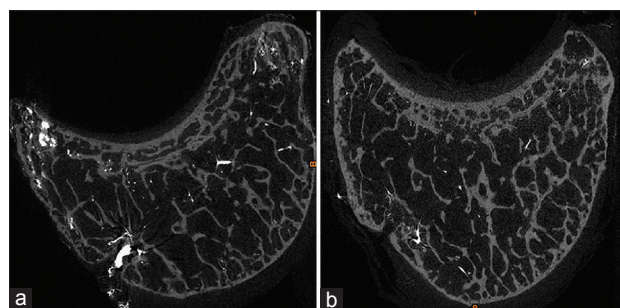


Figure 1: Reconstructed micro-computed tomography scanning images showing the nutrient foramina with enhanced arteries (a) and without enhanced arteries (b).

Table 1: The total number of nutrient foramina and the number of nutrient foramina with enhanced arteries (N = 6)

Items	Samples, n						Median	Z	P
	1	2	3	4	5	6			
Total number									
Palmar	2	2	2	2	2	1	2.00 (1.75, 2.00)	-1.807	0.071
Dorsal	3	1	5	3	4	4	3.50 (2.50, 4.25)		
With arteries									
Palmar	2	2	1	0	1	1	1.00 (0.75, 2.00)	-1.913	0.056
Dorsal	3	1	4	2	4	4	3.50 (1.75, 4.00)		

Data were presented as median (Q_1 , Q_3).

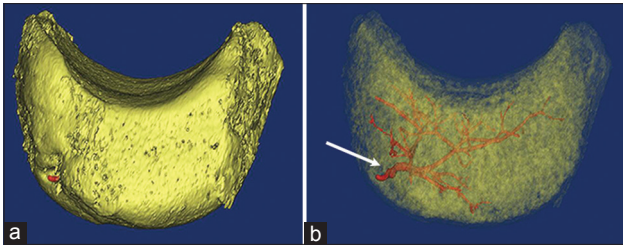


Figure 2: Reconstructed three-dimensional model of the Type A intraosseous arterial pattern. (a) The overall appearance of the lunate. (b) The intraosseous arteries in the same perspective, with the stems (arrow) from the palmar side.

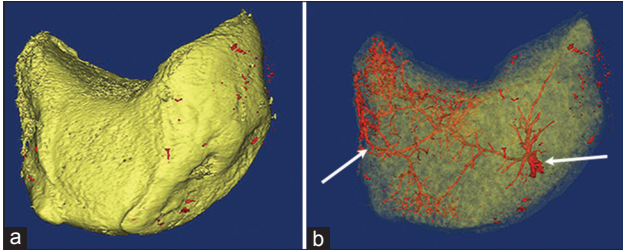


Figure 4: The Type C intraosseous arterial pattern. (a) The overall appearance of the lunate. (b) The intraosseous arteries, with the stems (arrows) from bilateral sides with anastomosis on the horizontal midline or lightly dorsal, in the same perspective.

with anastomosis. In the lunates of Type C, the stems from bilateral sides anastomosed in the central segment of lunates, and the anastomotic site was on the horizontal midline or slightly distal [Figure 4].

DISCUSSION

Many scholars concentrated on the intraosseous arterial pattern of lunates.^[1,2,11,12] Gelberman *et al.*^[11] defined a classic classification of intraosseous vascular pattern of normal lunates: X (10%), Y (59%), and I (31%) types. But, we do not think that Gelberman's classification is completely accurate. The pattern of single stems of lunate in our study cannot be classified with Gelberman's classification. Furthermore, this classification does not emphasize the dominant side of the blood supply and has some limitations in clinical applications.

The Spalteholz method is a classical anatomic study technique, making the tissue transparent to observe the intraosseous structures. The disadvantages are complicated steps and longtime spending. The steps include decalcification, dehydration, and transparency,^[2,11] which usually take 4–6 weeks. In addition, the study results are difficult to preserve even with batch processing and there are some limitations for researchers to observe the 3D vascular morphology of specimens by relying on photographs.

Micro-CT has a great advantage in studying trabecular bony structures. Several researchers^[8,9,13] have studied the structure of trabecular bones in normal and KD lunates to investigate the differences of structural characteristics and strength between them. However, these studies did not investigate

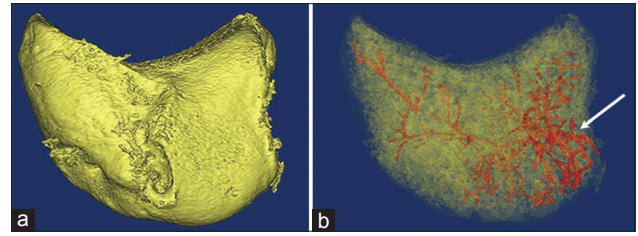


Figure 3: The Type B intraosseous arterial pattern. (a) Overall appearance of the lunate. (b) The intraosseous arteries in the same perspective, with the stems (arrow) from dorsal side.

the vessels and blood supply. Pb_3O_4 injection technique is commonly used for studying the microcirculation^[4,5] in reconstructive surgery. Angiography with micro-CT^[14,15] has been maturely applied to study the vascular distribution of small-sized samples such as rats. We propose that the Pb_3O_4 angiography with micro-CT could study the intraosseous arteries of lunates or the microvascular anatomy in other bones in the hand and wrist. Maybe with further improvement of micro-CT and contrast agents, this method could be applied to study the intraosseous arteries *in vivo*.

The injection method from low to high concentrations of Pb_3O_4 suspensions guarantees the reliability of micro-arterial filling. The injected stems and major branches of intraosseous arteries were clear and easily identified. This method is operationally simply, time-saving (usually within 3–5 days), and easy for handling batch specimens. In addition, the study utilized digital analysis to facilitate observation, data storage, following measurements, and analysis. However, lead oxide is toxic. Stringent personal protective equipment protocols are required for the use of lead oxide, and any residues and contaminated equipment require specialist disposal.^[15] Although the result shows a good reliability and validity, a preliminary experiment is suggested for operators to determine the appropriate sense of pressure in manual injection. Pressure-controlled pump could provide stable injection pressure. However, because of absence of feedback sense of injection, the differences of manual and mechanized injection still need further investigation.

There were no significant differences regarding the number of nutrient foramina between the palmar and dorsal sides, no matter whether total numbers or numbers with enhanced arteries. Obviously, a larger sample size will be helpful to get more conclusions, and the study of sample of Stage I KD will help to clarify the relationship between intraosseous vessels and the development of the lesion. In addition, we assume that this method can be applied to *in vivo* trials with the improvement of contrast agents, which requires further studies. Since the granules of grinded Pb_3O_4 cannot pass through the capillary vessels, our method could only illustrate fine arteries. For the nutrient foramina without enhanced arteries, Pichler and Putz^[16] studied the venous drainage of the lunate bone with epoxy injection through an artificial intraosseous canal, which suggested that there might be veins and/or nerves passing through the nutrient foramina without enhanced arteries. We assume that the

immunohistochemical method may contribute to the further study of these structures.

Acknowledgment

The authors thank Dr. Edward C. Mignot, Shandong University, for linguistic advice.

Financial support and sponsorship

This study was supported by a grant from Peking University Medicine Information Foundation (No. BMU20160600).

Conflicts of interest

There are no conflicts of interest.

REFERENCES

1. Lee ML. The intraosseous arterial pattern of the carpal lunate bone and its relation to avascular necrosis. *Acta Orthop Scand* 1963;33:43-55.
2. Panagis JS, Gelberman RH, Taleisnik J, Baumgaertner M. The arterial anatomy of the human carpus. Part II: The intraosseous vascularity. *J Hand Surg Am* 1983;8:375-82.
3. Bergeron L, Tang M, Morris SF. A review of vascular injection techniques for the study of perforator flaps. *Plast Reconstr Surg* 2006;117:2050-7. doi: 10.1097/01.prs.0000218321.36450.9b.
4. Rees MJ, Taylor GI. A simplified lead oxide cadaver injection technique. *Plast Reconstr Surg* 1986;77:141-5.
5. Pan WR, Cheng NM, Vally F. A modified lead oxide cadaveric injection technique for embalmed contrast radiography. *Plast Reconstr Surg* 2010;125:261e-2e. doi: 10.1097/PRS.0b013e3181d45eb4.
6. Xiao ZR, Xiong G, Guo SG, Du CC, Zhang YL. Microstructure study of normal lunates with micro-computed tomography. *J Huazhong Univ Sci Technolog Med Sci* 2017;37:384-389. doi: 10.1007/s11596-017-1744-6.
7. Yu DG, Nie SB, Liu FX, Wu CL, Tian B, Wang WG, *et al.* Dynamic alterations in microarchitecture, mineralization and mechanical property of subchondral bone in rat medial meniscal tear model of osteoarthritis. *Chin Med J* 2015;128:2879-86. doi: 10.4103/0366-6999.168045.
8. Han KJ, Kim JY, Chung NS, Lee HR, Lee YS. Trabecular microstructure of the human lunate in Kienbock's disease. *J Hand Surg Eur Vol* 2012;37:336-41. doi: 10.1177/1753193411422337.
9. Low SC, Bain GI, Findlay DM, Eng K, Perilli E. External and internal bone micro-architecture in normal and Kienböck's lunates: A whole-bone micro-computed tomography study. *J Orthop Res* 2014;32:826-33. doi: 10.1002/jor.22611.
10. Xiong G, Xiao Z, Wang H, Guo S, Tao J. Microstructural study of the lunate in stage III Kienböck's disease with micro-computed tomography imaging. *J Hand Surg Eur* 2016;24. [Epub ahead of print].
11. Gelberman RH, Bauman TD, Menon J, Akeson WH. The vascularity of the lunate bone and Kienböck's disease. *J Hand Surg Am* 1980;5:272-8.
12. Gelberman RH, Panagis JS, Taleisnik J, Baumgaertner M. The arterial anatomy of the human carpus. Part I: The extraosseous vascularity. *J Hand Surg Am* 1983;8:367-75.
13. Owers KL, Scougall P, Dabirrahmani D, Wernecke G, Jhamb A, Walsh WR, *et al.* Lunate trabecular structure: A radiographic cadaver study of risk factors for Kienböck's disease. *J Hand Surg Eur Vol* 2010;35:120-4. doi: 10.1177/1753193409103732.
14. Ghanavati S, Yu LX, Lerch JP, Sled JG. A perfusion procedure for imaging of the mouse cerebral vasculature by X-ray micro-CT. *J Neurosci Methods* 2014;221:70-7. doi: 10.1016/j.jneumeth.2013.09.002.
15. Kingston MJ, Perriman DM, Neeman T, Smith PN, Webb AL. Contrast agent comparison for three-dimensional micro-CT angiography: A cadaveric study. *Contrast Media Mol Imaging* 2016;11:319-24. doi: 10.1002/cmml.1695.
16. Pichler M, Putz R. The venous drainage of the lunate bone. *Surg Radiol Anat* 2003;24:372-6. doi: 10.1007/s00276-002-0065-y.